Hindawi
Applied Computational Intelligence and Soft Computing
Volume 2022, Article ID 4032419, 15 pages
https://doi.org/10.1155/2022/4032419

Research Article

Direction of Arrival Estimation for Coherent Signals' Method Based on LSTM Neural Network

Thanh Han-Trong,[1] **Nam Ngo Duc**,[1] **Hung Tran Van**,[1] **and Hung Pham-Viet**[2]

[1]*School of Electrical and Electronic Engineering, Hanoi University of Science and Technology, Hanoi 100000, Vietnam*
[2]*Faculty of Electrical-Electronics Engineering, Vietnam Maritime University, Haiphong, Vietnam*

Correspondence should be addressed to Hung Pham-Viet; phamviethung@vimaru.edu.vn

Received 28 February 2022; Revised 11 May 2022; Accepted 18 May 2022; Published 29 June 2022

Academic Editor: Abidhan Bardhan

Radio direction finding system is a system that determines the direction or coordinates of radio signal sources. The main function of this system is to determine the direction of arrival (DOA) of an incident radio wave. DOA information plays an important role in array signal processing and has many applications in communications, radar, seismic survey, etc. In this study, we propose a method to estimate the DOA by using the simulated signal dataset obtained at the linear antenna array (ULA) and the suitable Long Short-Term Memory (LSTM) network model. The performance of the method is evaluated based on the root mean square error (RMSE) parameter and then is compared with 2 other algorithms, multiple signal classification (MUSIC) and deep neural network (DNN) in different cases such as deviation of incoming signals, variation of signal-to-noise ratio (SNR), and coherent incoming signals. The obtained results have shown that the proposed method has significantly improved accuracy compared to other methods.

1. Introduction

For a long time, the problem of determining DOA has been a common problem in radio communication systems, radar systems [1], and navigation systems in air and waterway traffic [2]. These systems often use antenna arrays such as uniform linear antenna array (ULA), uniform circular antenna array (UCA), and uniform rectangular antenna array (URA) [3]. Many methods and algorithms have been researched and deployed to calculate DOA such as MUSIC [4–7], ESPRIT [8], total forward-backward matrix pencil [9, 10], and acoustic vector sensor [11]. They are also continuously developed to improve performance in DOA estimation for accuracy, resolution, and adaptability in the case of a limited number of snapshots, low signal-to-noise ratio (SNR), signal-to-noise correlation, etc.

In recent years, the application of artificial intelligence techniques in the DOA estimation problem has been concerned. Network models have been applied to improve accuracy and speed in DOA calculations [12, 13]. The deep learning methods do not need to calculate the signal characteristics during the prediction process, so the real-time estimation process will be shortened thereby providing higher real-time applicability such as support vector regression (SVR) [14, 15] and support vector machine (SVM) [16, 17]. In deep neural network (DNN) [12, 18], convolution neural network (CNN) [13, 19–21] and Adam optimal function were used to estimate DOA with satisfactorily accurate results. Also, radial basis function neural network (RBFNN) [22] can estimate the DOA with good accuracy under favorable environmental conditions.

This study focuses on the research and development of a simulation database of the signals received from the ULA antenna array. From the obtained dataset, the suitable long-short term memory (LSTM) algorithm is proposed to be applied to calculate the DOA of incoming signals which are coherent. The received results will be evaluated and compared with other typical methods to assess the performance of the proposed method.

The study is organized as follows. Section 2 introduces the summary of research results on DOA calculation that have been done previously. Section 3 presents the antenna

array model, the method of simulating the signal received at the antenna array, and the applied algorithm model. Section 4 shows the experimental results and gives evaluation for each algorithm. Conclusions and future work are in Section 5.

2. Related Work

Table 1 summarizes several methods of estimating the DOA based on the signal spectrum. These included both correlated and uncorrelated signals. They are divided into two categories: using machine learning algorithms and using classical algorithms. The classical algorithm based on multisignal classification can predict accurately, but the computational complexity is high. One of the most commonly used classical algorithms is MUSIC which was discovered by independent studies of Schmidt [23] and Bienvenu [24]. The music algorithm has been shown to work well when the signals are uncorrelated, the incoming signal sources are far apart and the SNR is large enough. Specifically, with the antenna array ULA, MUSIC can estimate the DOA of 2 signals at -5° and 5° with RMSE $\approx 0.7^{\circ}$ for SNR $= -10$ dB and RMSE $\approx 0.05^{\circ}$ SNR ≈ 10 dB [5]. However, when the signal sources are correlated, the performance of the MUSIC algorithm is not good. Since then, the improved MUSIC algorithms have been studied to determine the DOA of correlated incoming signals with the reduced number of calculations, such as IMMUSIC and MMUSIC [4] or using the covariance matrix with the transpose elements [5]. However, if there are more three correlated incoming signals, classical algorithms still need to improve and develop. In addition, algorithms are often developed with the assumption that the number of incoming sources is known [5, 8, 9], which reduces the generality of the problem and is no longer true when applied in practice because the signal received at the antenna array is the total signal of many unknown and unstable incoming sources.

Several recent publications have shown that machine learning methods have gradually been applied to solve the problem of DOA estimation. Usually, convolutional neural network algorithms can extract the basic nonlinear structures of the input data. Therefore, CNN with a simple layer structure can estimate the DOA of uncorrelated sources [13, 19]. Because of its simple structure, the CNN network performs DOA estimation with large bandwidth quickly and efficiently, thereby the DOA information can be calculated in real time.

CNNs are often trained with large amounts of data where suitable data are fed into the network when they have almost the same distributions, including both training and testing data [25, 26]. In fact, besides DOA information, the received signal model at the antenna array includes many unknown parameters such as the number of incoming sources, frequency, and signal-to-noise ratio. Signals received from the antenna array will be preprocessed to reduce their distribution divergence before becoming input data of the DNN [12, 18]. The output of a DNN network [18, 27] is usually as an angular grid, corresponding to each position in the angular grid representing the spectral value of the signal. If the angle of incidence coincides with the angle present in the mesh, then the DOA problem can be estimated correctly. However, the angles present in the mesh cannot match the actual DOA angle completely. The authors in [19] describe the construction of the network in 2 stages, in which the first stage performs the estimation with the grid of angles. The second stage corrects the difference between the DOA and the discrete angle in the nearest mesh, thus resolving the disparity caused by the discrete angle. Specifically, this study estimates 2 narrowband and uncorrelated incoming signals at the ULA antenna array. The number of antennas in the array is 8 with the number of snapshots being 256. The DOA was estimated with RMSE $\approx 0.11^{\circ}$ at SNR $= 5$ dB and RMSE $\approx 0.05^{\circ}$ at SNR $= 10$ dB. However, the research results of this study still need to be improved to be able to estimate DOA in cases where there are more than 2 incoming signals as well as in cases correlated incoming signals.

Besides using RNNs for applications related to natural language processing such as speech recognition, RNN networks are also used for DOA estimation [28–30]. In [30], the RNN is created based on bidirectional long-short term memory (BiLSTM). RNNs do not directly estimate DOA but classify them based on classes.

In those classes, the incident angles are in the range $[0^{\circ}, 90^{\circ}]$ with angular deviations of the incoming sources being 10°, 5°, 2°, 1°, respectively. This study for the estimation of DOA has quite good results. However, similar to the previously presented DNN algorithm, the RNN is dependent on the angular grid for classification and the performance of this method is still degraded at low SNR.

In [31], the LSTM network is also used to determine the DOA. With LSTM networks, it is suitable for nonstationary targets because it can be generalized to learn sequential patterns. The LSTM network is presented in more detail in [32]. In the unknown multipath environment, it is necessary to estimate the DOA for a moving target using the LSTM-based "New Multi-frame Phase Enhancement" technique, in which the recommended number of frames is 3, 5, and 7. In most cases, when conducting surveys under the same environmental conditions, the larger the number of frames, the better the accuracy. For example, the signal received at the ULA antenna array-comprising 21 elements with distanced $d = 0.5\lambda$, SNR $= -10$ dB, and wavelength $\lambda = 1$ m, using the estimated network got RMSE values of 0.24°, 0.27°, and 0.32° which correspond to $k = 7, 5, 3$. The increase in frame weight increases the accuracy of DOA estimation but reduces the performance of the problem. Therefore, depending on the environmental conditions, the system must choose the appropriate number of frames. Although the results are quite good, the problem still encounters obstacles when the incoming sources are correlated. To improve on the DOA problem when the incoming sources are correlated signals and the angular deviations of the signal sources are small, this study proposes an LSTM network with a simpler model consisting of fully connected layers, excluding frame, to estimate the direction of the incoming signal. The obtained model will be compared with DNN and LSTM algorithms through the RMSE parameter presented in Section 3.

Table 1: Methods of estimating the DOA based on the signal spectrum.

Author	Method	Objective	Dataset
Yan Gao et al, 2014	MUSIC	An improved music algorithm for DOA estimation of coherent signals	N/A
Zhang-Meng Liu et al., 2018	DNN	Direction-of-arrival estimation based on deep neural networks with robustness to array imperfections	19800 samples
Wenli Zhu et al., 2019	CNN	A deep learning architecture for broadband DOA estimation	144000 samples
Min Chen et al., 2020	DNN	Deep neural network for estimation of direction of arrival with antenna array	121000 samples
Georgios K. Papageorgiou et al., 2020	CNN	Deep networks for direction-of-arrival estimation in low SNR	36300 samples
Van-Sang Doan, Dong-Seong Kim, 2020	MUSIC	DOA estimation of multiple noncoherent and coherent signals using element transposition of covariance matrix	N/A
M. Wajid, B. Kumar, A. Goel, A. Kumar and R. Bahl, 2020	RNN	Direction of arrival estimation with uniform linear array based on recurrent neural network	N/A
Hyeonjin Chung et al., 2021	CNN & DNN	Off-grid DoA estimation via two-stage cascaded neural network	106800 samples
Houhong Xiang et al, 2021	LSTM	Improved direction-of-arrival estimation method based on LSTM neural networks with robustness to array imperfections	150000 samples

3. Materials and Methods

3.1. Uniform Linear Antenna Array and Signal Model. This study uses a uniform linear antenna array (ULA) with M elements. The structure of the ULA antenna array is shown in Figure 1. The element in the antenna system acts as an omnidirectional source. These antenna elements operate in phase with each other to create a unique radiation direction so that the signal sent to the processor is kept in phase and amplitude in comparison with the incoming signal. Furthermore, the ULA antenna array has several advantages over other types of antenna arrays as shown in [3, 9].

Assuming that the incoming signal is in the same azimuth plane as the antenna array, the signal transmitted to the antenna array is illustrate as Figure 1.

The antenna array (ULA) used in this study has M elements, equally spaced with a distance of d. Assume that the system has K incoming signal sources with wavelength λ. The received signal at each antenna element is the sum of all incoming signals at the same time. The mathematical representation of the signal received at the m_{th} antenna element is described as in Equation.(1), where $s_k(t)$ and θ_k are the complex amplitude and the DOA of the k_{th} source $(k = 1, 2, \ldots, K)$, respectively:

$$x_m(t) = \sum_{k=1}^{K} s_k(t) e^{-j(2\pi/\lambda)(m-1)d \sin \theta_k} + n_m(t), \tag{1}$$

where $m = 1, 2, \ldots, M$ and $n_m(t)$ is the noise received at the m_{th} antenna element of the array.

Define A is a matrix of size $M \times K$ including the elements represented as follows:

$$a_{m,k} = e^{-j(2\pi/\lambda)(m-1)d \sin \theta_k}. \tag{2}$$

Therefore, Equation (1) can be rewritten as

$$x(t) = \mathrm{A}s(t) + n(t), \tag{3}$$

where $x(t)$, $n(t)$, and $s(t)$ are defined by

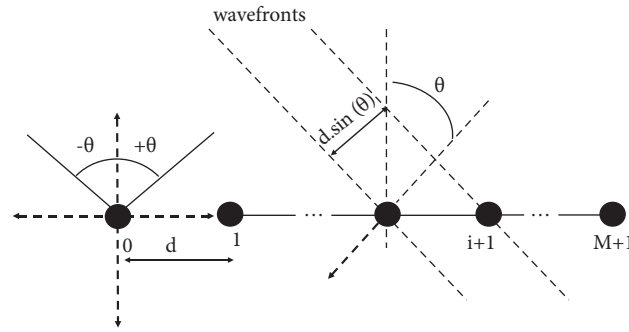

Figure 1: Model of uniform linear antenna array.

$$\begin{aligned} x(t) &= [x_1(t), x_2(t), \ldots, x_M(t)]^T, \\ s(t) &= [s_1(t), s_2(t), \ldots, s_K(t)]^T, \\ n(t) &= [n_1(t), n_2(t), \ldots, n_M(t)]^T, \end{aligned} \tag{4}$$

where T is the transpose of the matrix.

In [16, 33], the signals received at the antenna array will be passed through a preprocessor before being processed to calculate DOA information. Therefore, the correlation matrix of size $M \times M$ of the received signals at the antenna array can be represented as follows:

$$R_{xx} = E\left[x(t)\, x^H(t)\right] = \mathrm{ASA}^H + R_n, \tag{5}$$

where $E[\cdot]$ and $[\cdot]^H$ are the expectation and the Hermitian transpose, respectively, and S and R_N are correlation matrices of size $K \times K$ of signal and noise, respectively, and are represented as follows:

$$S = E\left[s(t) s^H(t)\right], \tag{6}$$

$$R_n = E\left[n(t) n^H(t)\right]. \tag{7}$$

From there, Equation (2) can be rewritten as

$$R_{xx} = \mathrm{ASA}^H + \sigma^2_{\text{noise}} I, \tag{8}$$

where I is an identity matrix of size $M \times M$ and σ^2_{noise} is the noise power. The correlation matrix is also called as the Hermitian matrix. This matrix is used as input for the DOA estimation models.

3.2. DOA Estimation

3.2.1. Recurrent Neural Network. Deep learning has two major models: convolutional neural network (CNN) for problems with image input and recurrent neural network (RNN) for sequence data problems.

Recurrent neural network is a model that uses memory to store information from previous computation steps and makes an accurate prediction for the current prediction step. Consider the "many to many" RNN model, as shown in Figure 2.

Figure 2 shows that the input x_t will be combined with the previously hidden layer h_{t-1} using the function f_w to compute the hidden layer h_t and the output y_t. W is the set of weights added to all activation functions. Loss functions $L_1, L_2, \ldots, L_t$ are to calculate the difference in the output from the actual value. The smaller the value of the loss function, the more accurate the result.

Recurrent means that the model will perform identical calculations for each element of the input data series, and the output will depend on the results of the previous calculations. Here, the RNN only uses a single neural network (usually a layer) to calculate the output value in each time step. Therefore, the outputs converted to inputs will be multiplied by the same weight matrix (here, W as shown in Figure 2). It is also why there is the word Recurrent in the name of the RNN.

3.2.2. Long Short-Term Memory Networks. Long short-term memory (LSTM) is an artificial recurrent neural network that takes the form of a sequence of repeating modules and contains feedback connections. This network is often used in problems where the input is a data string such as speech or video. Figure 3 shows the structure of multilayer LSTM networks.

With the network depicted in Figure 3, the LSTM network nodes in the same layer connect in a chain form and connect to the corresponding nodes in the next layer. An LSTM unit consists of an input and an output port. They have a 4-layer structure that interacts with each other in a very specific way as depicted in Figure 4.

The general parameters of the network model have been described in [31]. Specifically, in the t^{th} state of the LSTM model, the classic LSTM module structure includes input c_{t-1}, h_{t-1} are the outputs in the $(t-1)^{\text{th}}$ state, and x_t is the input in the t^{th} state of the model. Output includes c_t, h_t, where c_t is called cell state and h_t is hidden state at t^{th} state:

$$f_t = \sigma\left(W_f^* x_t + W_f^* h_{t-1} + b_f\right), \tag{9}$$

$$i_t = \sigma\left(W_i^* x_t + W_i^* h_{t-1} + b_i\right), \tag{10}$$

$$o_t = \sigma\left(W_o^* x_t + W_o^* h_{t-1} + b_o\right), \tag{11}$$

$$\widetilde{c}_t = \tanh\left(W_c^* x_t + W_c^* h_{t-1} + b_c\right), \tag{12}$$

$$c_t = f_t^* c_{t-1} + i_c^* \widetilde{c}_t + b_c, \tag{13}$$

$$h_t = o_t^* \tanh\left(c_t\right), \tag{14}$$

where f_t is the forget gate, $0 < f_t, i_t$ is input gate, o_t is output gate, $o_t < 1$, b_f, b_i, b_o are the bias coefficients, and W is the weight matrix.

This study proposes an LSTM model for the DOA problem, as shown in Figure 5. This network is designed with one input layer, three LSTM layers, three fully connected layers, and one output layer. Relu activation function is used at the output of each layer fully connected. In the output layer, we use the linear activation function. The signal received at the antenna array is processed at the preprocessing unit to obtain the correlation vector. That correlation vector is the input to the LSTM network. The output layer with n elements is used to estimate the DOA. A detailed description of the classes is shown in the following section.

For the fully connected layer, the nodes in the former layer are connected to all the nodes in the following layer with their coefficients w. Each node has its bias coefficient b. Each node in the fully connected, and output layer performs two steps: linear summation and applying the activation function, as shown in equations (15) and (16). Assume the number of nodes in the fully connected i^{th} is $l^{(i)}$. The matrix $W^{(k)}$ of size $l^{(k-1)} \times l^k$ is the coefficient matrix between layer $(k-1)$ and layer k, where $w_{ij}^{(k)}$ is the connection coefficient from the i^{th} node of layer $k-1$ to the j^{th} node of layer k. Vector $b^{(k)}$ of size $l^k \times 1$ is the bias coefficient of the nodes in layer k, where $b_i^{(k)}$ is the bias of the i^{th} node in layer k.

Step 1 (linear summation): this is the sum of all nodes in the previous layer multiplied by the corresponding w factor plus the bias b:

$$z_i^{(k)} = \sum_{j=1}^{l^{(l-1)}} a_j^{(l-1)} * w_{ji}^{(l)} + b_i^{(l)}. \tag{15}$$

Step 2: applying activation function,

$$a_i^{(l)} = h\left(z_i^{(l)}\right), \tag{16}$$

where h is the activation function, vector $z^{(k)}$ of size $l^{(k)} \times 1$ is the value of nodes in layer k after the linear summation step. Vector $a^{(k)}$ of size $l^{(k)} \times 1$ is the value of nodes in layer k after applying the activation function.

3.2.3. Data Preprocessing. The LSTM network is trained with a large amount of data. In order to reduce the input bias and variation of the signal, the signal preprocessing is carried out with the input signal received at the antenna array and the output as a correlation matrix R_{xx} of size $M \times M$:

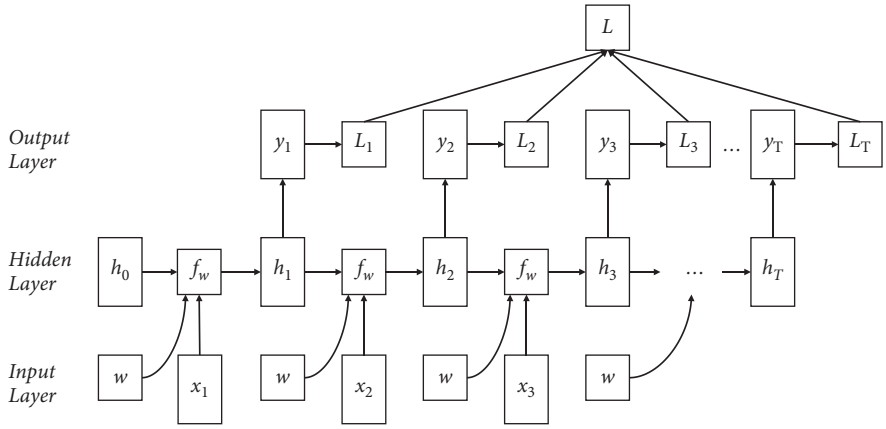

Figure 2: RNN Model "many to many."

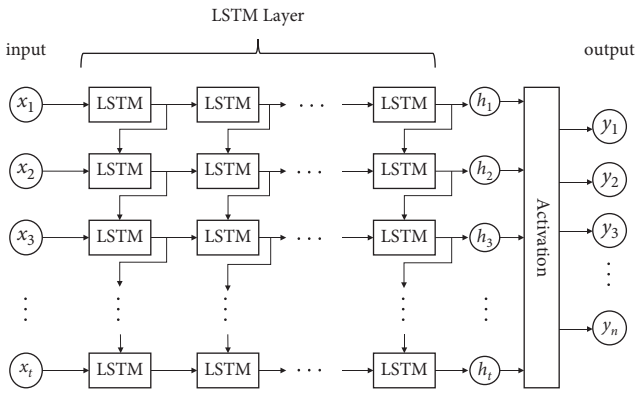

Figure 3: Multilayer LSTM network structure.

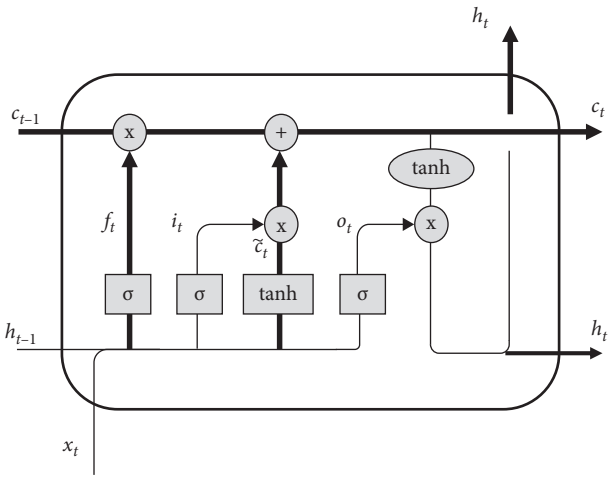

Figure 4: Structure of the LSTM module.

$$R_{xx} = \begin{bmatrix} r_{1,1} & r_{1,2} & \cdots & r_{1,M} \\ r_{2,1} & r_{2,2} & \cdots & r_{2,M} \\ \vdots & \vdots & \ddots & \vdots \\ r_{M,1} & r_{M,2} & \cdots & r_{M,M} \end{bmatrix}. \quad (17)$$

Since R_{xx} is a Hermitanian matrix, the upper triangular matrix and the lower triangular matrix carry the same information. According to the methods published in [12, 34], the upper triangular matrix has enough information to compute the DOA. Therefore, to reduce the amount of information for the input of the network, this study only uses the upper triangular matrix of R_{xx} and then transforms it into a vector r of length $M \times (M-1)$:

$$r = \left[R\left(r_{1,2}\right), R\left(r_{1,3}\right), \ldots, R\left(r_{M-1,M}\right), I\left(r_{1,2}\right), I\left(r_{1,3}\right), \ldots, I\left(r_{M-1,M}\right)\right]T, \quad (18)$$

where $r_{i,j}$ is the $(i, j)^{\text{th}}$ element in the matrix R_{xx}. Since $r_{i,j}$ is a complex number, it cannot be put directly into the network for calculation. Therefore, before putting into the training network, each element $r_{i,j}$ will be represented into 2 components, the real part $R(.)$ and the imaginary part $I(.)$.

3.2.4. Data Generation. In this section, a general method to generate data for the training model for the case of multiple incoming sources is proposed. Suppose there are K sources to the M elements ULA antenna array-($K < M$). The angles $\theta_1, \theta_2, \ldots, \theta_{K-1}, \theta_K$ correspond to K incoming sources in the range $[\theta_{\min} \div \theta_{\max}]$. The values $\Delta_1, \Delta_2, \ldots, \Delta_{K-1}$ are defined, respectively, as the difference between the incoming sources, where Δ_1 is the difference between the first and the second incoming signals, Δ_{K-1} is the difference between the $(K-1)^{\text{th}}$, and the K^{th} incoming signals with $\theta_{\min} \le \theta_1 \le \theta_{\max} - (\Delta_1 + \cdots + \Delta_{K-1})$. Then, the DOA of the first source is θ_1, then the DOA of 2^{nd} source, 3rd... and K^{th}, respectively, is $\theta_2 = \theta_1 + \Delta_1, \theta_3 = \theta_1 + \Delta_1 + \Delta_2, \ldots, \theta_K = \theta_1 + \Delta_1 + \Delta_2 + \cdots + \Delta_{K-1}$, and then the signal $x(t)$ received at the antenna array is calculated as in Equations (1) and (4).

For data generation process, when the DOA of the first signal θ_1 is sampled in the range $[\theta_{\min}, \theta_{\max} - (\Delta_1 + \cdots + \Delta_{K-1})]$ with a jump of Δs°, the DOA of signal 2^{nd}... and K^{th}, respectively, are $\theta_1 + \Delta_1 \ldots$ và $\theta_1 + \Delta_1 + \Delta_2 + \cdots + \Delta_{K-1}$. From there, the total amount of generated data is calculated by the following formula:

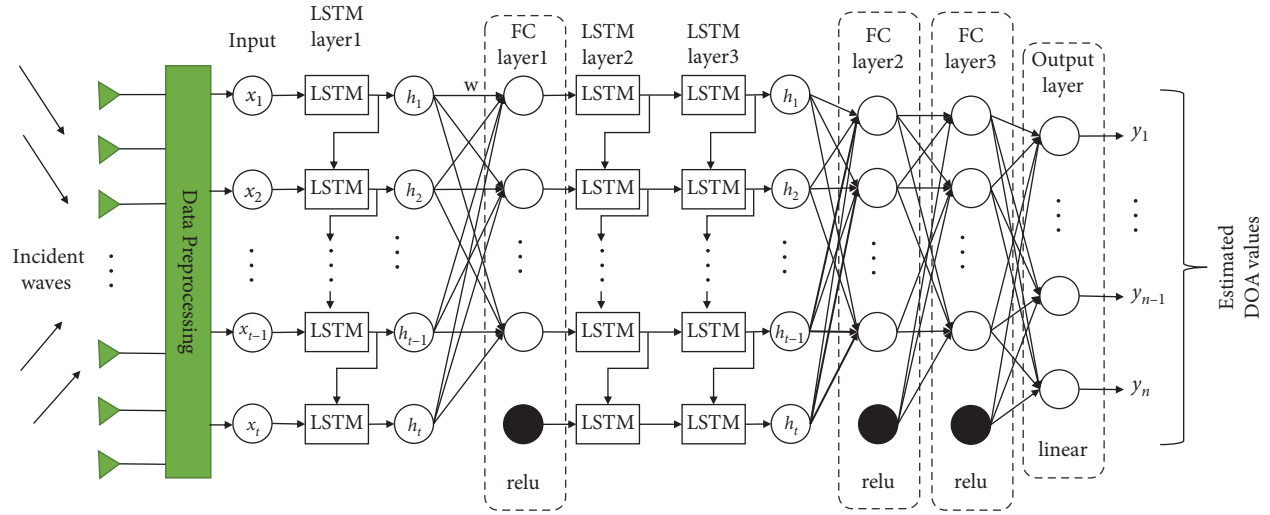

Figure 5: Proposed LSTM network model for DOA estimation.

$$\text{data}_{\text{sum}} = \frac{\left(\theta_{\max} - \left(\Delta_1 + \cdots + \Delta_{K-1}\right) - \theta_{\min}\right)}{\overset{s^{\circ}}{\Delta}} + 1. \tag{19}$$

3.2.5. Data Labeling. The input is defined as vector $r(\theta_1, \theta_2, \ldots, \theta_K)$ as Equation (18), where K is the number of incoming signals, corresponding to the incoming signals at the angles $(\theta_1, \theta_2, \ldots, \theta_K)$.

In this study, a labeling method called one hot encoding with multiple labels is used to label the data. $[y(\theta_1, \theta_2, \ldots, \theta_K)]_{\text{label}}$ is the corresponding label of the incoming signals. With 121 outputs corresponding to incoming angles in the range $[-60^{\circ} \div 60^{\circ}]$ with a jump of 1°, $[y(\theta_1, \theta_2, \ldots, \theta_K)]_{\text{label}}$ is defined as

$$\left[y(\theta_1, \ldots, \theta_K)\right]_{\text{label}} = \begin{cases} 1, & \text{at } \theta_i \text{ with } i = 1, \ldots, K, \\ 0, & \text{otherwise.} \end{cases} \tag{20}$$

Therefore, the output of the LSTM network corresponding to the input $y(\theta_1, \theta_2, \ldots, \theta_K)$ is $y(\theta_1, \theta_2, \ldots, \theta_K)$

3.2.6. Evaluation Parameters. To evaluate the accuracy of two proposed models, this research uses two error functions: MSE and RMSE.

(a) MSE function: to evaluate the model during training, the network uses the mean square error loss (MSE) function. MSE is defined as

$$\text{MSE} = \frac{1}{n} \sum_{i=1}^{n} \left(y_i - \widehat{y}_i\right)^2. \tag{21}$$

(b) RMSE function: this study uses the root mean square error function (RMSE) to evaluate the performance of the model and algorithm:

$$\text{RMSE} = \sqrt{\frac{1}{\text{NK}} \sum_{k=1}^{K} \sum_{n=1}^{N} \left(\theta_k - \widehat{\theta}_{k,n}\right)^2}, \tag{22}$$

where K is the number of incident sources, N is the number of trials, and θ_k and $\widehat{\theta}_{k,n}$ are the incident angle of the source k_{th} and the estimated angle of k_{th} source at the n_{th} trial.

4. Experiments and Results

In this section, the results obtained from the LSTM method are presented in different cases and compared with some other DOA methods, such as Music and DNN.

4.1. Simulation Establishment. This study uses a 10-element ULA antenna array with $d = \lambda/2$. The incoming signal has a frequency of 2 GHz. The received signals must be narrowband in both correlated and noncorrelated cases; simulation data are generated according to Equation. (1) with SNR = 10 dB and snapshot = 400.

For the LSTM network, the size of each layer is shown in Table 2. Assume that the incoming signals are in the range $[-60^{\circ}, 60^{\circ}]$, with a jump of 1°. Therefore, the number of nodes of the output layer will be 121. The spatial spectrum is constructed with a grid of 1°, so there is a total of 121 grids with $\theta_1 = -60, \theta_2 = -59, \ldots, \theta_{121} = 60$. In this study, we use the spectral reconstruction method according to [18].

The training samples are generated by considering signals separated by Δ_θ. In this study, we assume that the number of incoming signals is one, two, and three, respectively. The details are shown in Table 3. The data generation process is mentioned in Section 3.2.4.

For the case of two incoming signals, when the DOA of the first signal is created by sampling in the range $[-60^{\circ}, 60^{\circ} - \Delta]$ with a jump of 1°, then the DOA of the second signal will be $\theta + \Delta$. In the case of three incoming signals, when the DOA of the first signal is created by sampling in the range $[-60^{\circ}, 60^{\circ} - \Delta_1 - \Delta_2]$ with a jump of 1°, the DOA of the second signal and 3^{rd} are $\theta + \Delta_1$ and $\theta + \Delta_1 + \Delta_2$, respectively. In the last case, with an incoming signal, the DOA of the signal is created by sampling in the range $[-60^{\circ}, 60^{\circ}]$ with a jump of 1°. The covariance vectors

Table 2: Number of nodes in each layer.

Class name	Number of nodes
LSTM1	256
FC1	90
LSTM2	256
LSTM3	256
FC2	200
FC3	128
Output	128

Table 3: Incoming signal cases.

Number of incoming signals	Cases	Angular distance
One incoming signal		
Two incoming signals	Two correlated signals	$\Delta_\theta = \{2, 4, \ldots, 10\}$
	Two uncorrelated signals	
Three incoming signals	Three correlated signals	
	Two correlated signals	
	Three uncorrelated signals	

are computed from the samples as input to the LSTM network according to Equation. (18) and the corresponding labels, as in Equation. (20). The SNR for incoming signals in all cases is 10 dB. For the training process, the learning rate is 0.001, the batch size is 1024, and the number of Epochs is 400. During the training, the network parameters are continuously updated to optimize the MSE loss function, as mentioned in Equation. (21). In addition, the network uses the ADAM optimization algorithm [35] to optimize the time and predictability of the algorithm.

4.2. Simulation Results

4.2.1. Uncorrelated Signal. In the first test, with SNR = 10 dB, we assume that the incoming signals are uncorrelated. All three algorithms with the same simulation setup conditions will be executed. With the LSTM network, the results shown in Figure 6 include the cases of 1 source (DOA = 10°), two sources (DOA of 20° and 26°), and three incoming sources (DOA of 30°, 36°, and 42°). In the above cases, the DOA can be well estimated. Specifically, in Figure 6(a), it is easy to see that the signal spectrum is quite simple because there is only one incoming source, LSTM gives the result MSE ≈ 0.0006°. In the remaining two cases, when the angular distance is 6°, the LSTM network can all estimate well with the signal spectrum separated by RMSE ≈ 0.0458°. With the DNN network and the MUSIC algorithms, it can be seen that the proposed LSTM network estimates the DOAs more accurately than the other two algorithms as well as the previous studies (CNN and LSTM). The signal spectrum is shown in Figures 7 and 8. It shows that the signal sources have not been separated.

In the next test, to evaluate the influence of SNRs on the accuracy of the algorithm, we apply the LSTM model to estimate the DOA when there are three incoming sources with angular difference $\Delta_\theta = 10°$. Considering 2 cases of SNR = 0 dB and SNR = −5 dB with 31 test samples, the results are shown in Figure 9. At SNR = 0 dB, the estimated angle is almost close to the actual angle. When SNR = −5 dB, although the estimated result differs slightly from reality, the LSTM model still gives good results with error <0.5°.

To clarify more clearly the influence of SNR on the performance of the LSTM network model in the case of one incoming signal, consider the SNR in the range [0 dB ÷10 dB]. The results are shown in Figure 10. It is easy to see that, in the case of 1 source to the antenna array, LSTM still gives better results than the other two methods with RMSE < 0.5°.

For the case of 2 incoming sources, consider the SNR in the range [0 dB ÷10 dB]. The results are shown in Figure 11. It can be seen that, with two incoming sources, the LSTM method still gives better results than the DNN and MUSIC networks.

When investigating the angle resolution of the proposed algorithm, we consider the case that there are two uncorrelated incoming signals with SNR = 10 dB at $\Delta_\theta = [2°, 4°, 6°, 8°, 10°]$. The results are shown in Tables 4–6, respectively, with LSTM, DNN, and MUSIC algorithms. From the results' tables, we can see that the LSTM model still works effectively and gives better results than the other two methods in both cases, where the signals are close to each other and far apart with RMSE < 0.06°.

4.2.2. Correlated Signal. With the correlated incoming signals, the MUSIC algorithm no longer works correctly [4, 5]. Therefore, the MUSIC-IMPROVE algorithm (according to the covariance matrix transpose method) and DNN are used to compare with the results obtained from the LSTM algorithm.

Test on two incoming signals with the DOA of 0° and6°, the same with three incoming signals at the DOA of 0°, 6°, and 12° The results are presented in Figures 12–14 for LSTM, MUSIC-IMPROVE, and DNN algorithms, respectively. Since the signal spectrum conspicuous to the

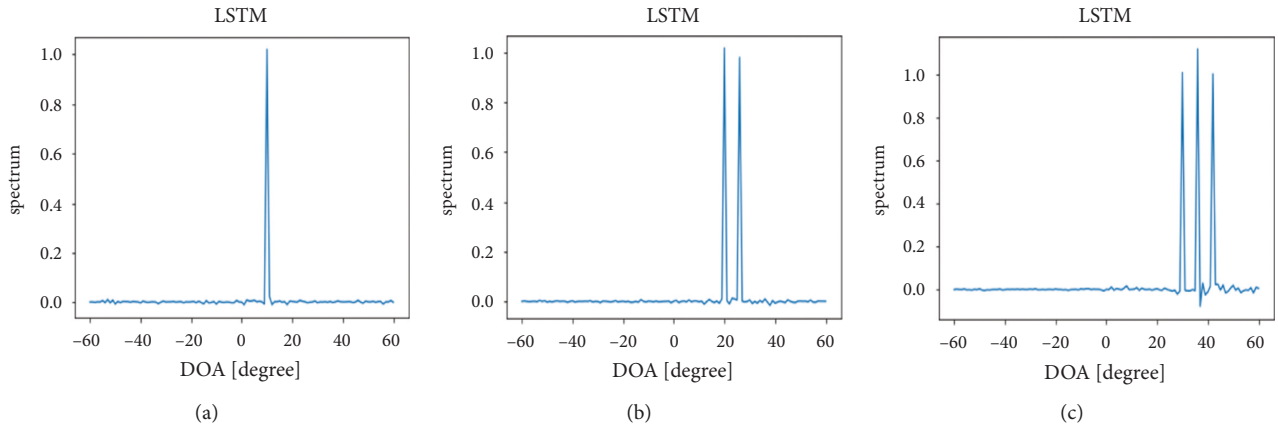

Figure 6: The signal spectrum of the incoming source is uncorrelated based on the LSTM method in the following cases: (a) 1 signal, **MSE** = **0.0006**°, (b) 2 signals, **RMSE** ≈ 0.0458°, and (c) 3 signals, **RMSC** = **0.0301**°.

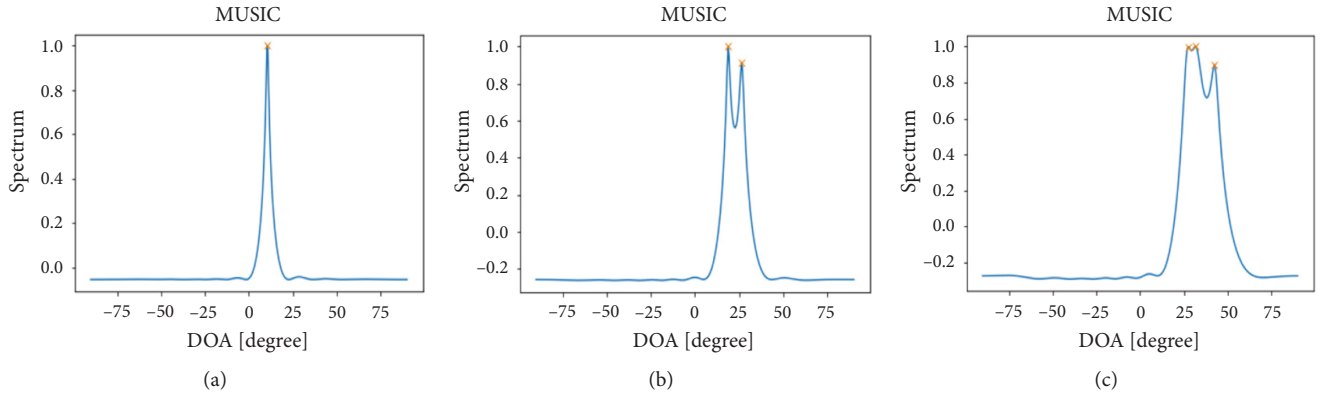

Figure 7: The signal spectrum of the incoming source is not correlated based on the MUSIC method in the following cases: (a) 1 signal **MSE** = **0.038**°, (b) 2 signals **RMSE** = **0.88**°, and (c) 3 signals **RMSE** = **2.97**°.

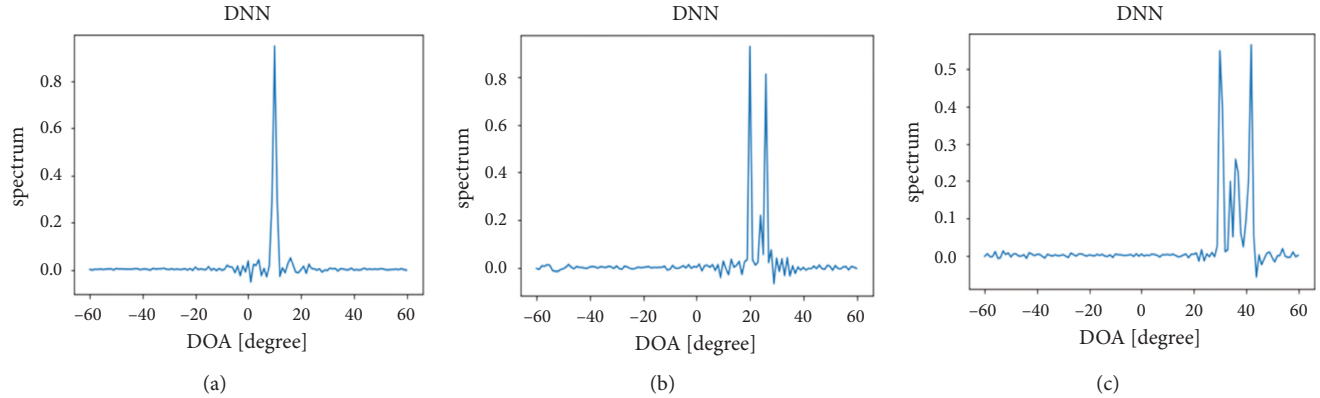

Figure 8: The signal spectrum of the incoming source is not correlated based on the DNN method in the following cases: (a) 1 signal **MSE** = **0.0023**°, (b) 2 signals **RMSE** = **0.28**°, and (c) 3 signals **RMSE** = **0.5**°.

incoming signal is two correlated signals, all three algorithms work well with a well-separated signal spectrum. When the incoming signal is over two, both MUSIC-IMPROVE and DNN give worse results, while the LSTM algorithm still works well.

To evaluate the resolution in this case, we assume that the three correlated incoming signals differ by in turn amount $\Delta_1 = \Delta_2 = \Delta_\theta$ degrees. Simulation results are shown in Table 7, while with two algorithms, MUSIC-IMPROVE and DNN, the estimated results are shown in Tables 8 and 9. Those tables show that the LSTM model still correctly predicts the DOA of many correlated incoming signals, while the MUSIC algorithm proves to be less efficient in this case. This can also be seen in Figure 13. Some results

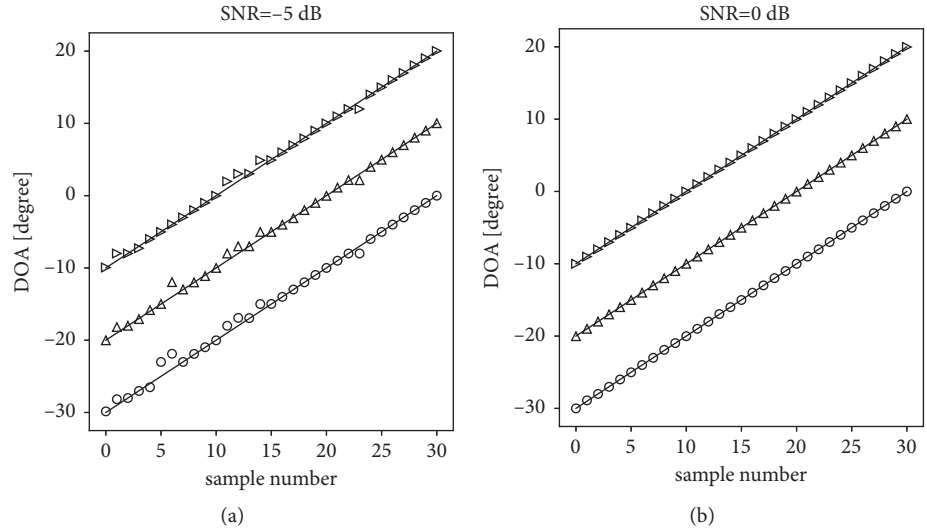

Figure 9: Comparison between the actual and estimated DOA values of the 3 signals of the LSTM method: (a) at SNR = −5 dB and (b) at SNR = 0 dB.

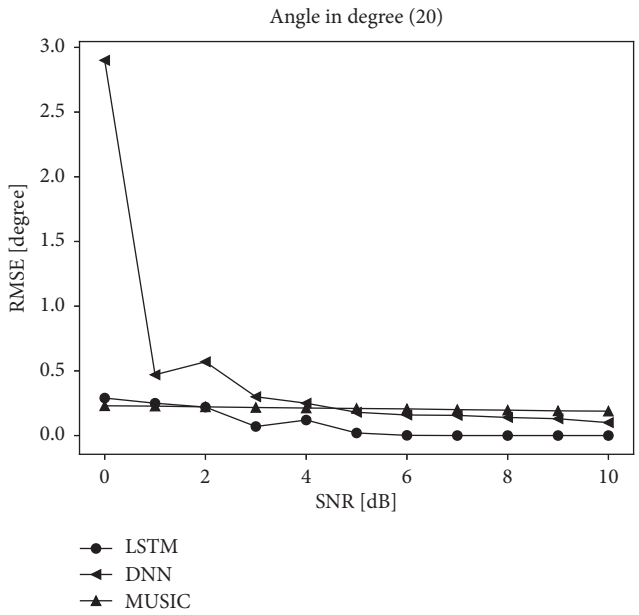

Figure 10: RMSE (degree) of proposed LSTM-based DOA estimation algorithm, standard MUSIC algorithm, and DNN method with different value SNRs at DOA of 20°.

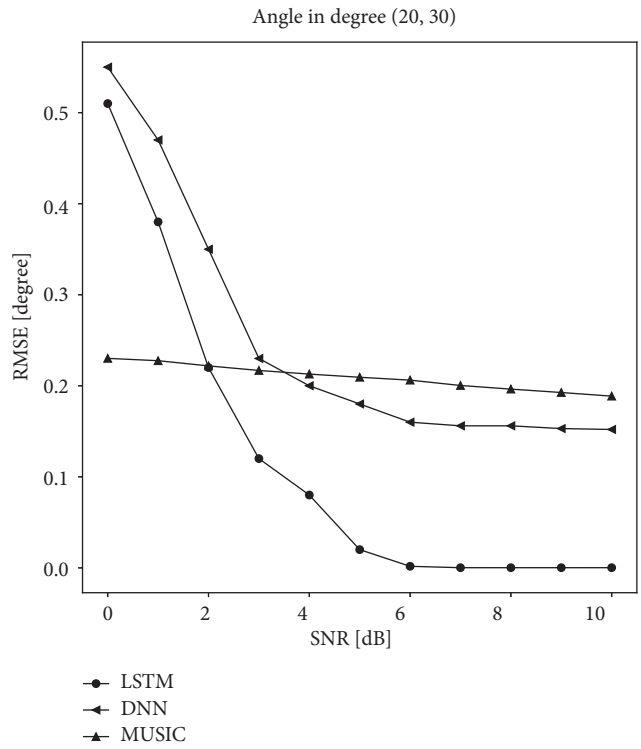

Figure 11: RMACTSE (degrees) of the proposed LSTM-based DOA estimation algorithm, the standard MUSIC algorithm, and the DNN method with different SNR values at the DOA of 20° and 30°.

published in [5] have also shown that some other improved MUSIC methods also give poor results in the case of correlated incoming signals. For the DNN model, with the difference among the incoming signals being small, the DNN method also gives poor results. The algorithm only works better when the difference among the incoming signals is large enough.

The next experiment will evaluate the effect of SNRs on the accuracy of the algorithm. In the case of two correlated incoming signals, consider the SNR in the range of [0 dB÷10 dB]; the results are shown in Figure 15. With the three correlated incoming signals and the SNR in the range of [−5 dB÷5 dB], the result depicted in Figure 16 indicates that, in both cases, the LSTM model gives the best results compared to the other two methods (in the case of SNR > 4 dB, RMSE ≈ 0).

Figure 17 shows the RMSE comparison results of the algorithms at the DOA (20°, 30°, 40°*s*), with the SNR in the

Table 4: Result of LSTM algorithm (SNR = 10 dB).

Δ_θ	Input (degree)		Output (degree)		RMSE (degree)
2°	30	32	29.97	32.06	0.05
4°	30	34	29.99	33.98	0.02
6°	30	36	30	35.98	0.02
8°	30	38	30	37.92	0.057
10°	30	40	30	40.01	0.007

Table 5: Result of MUSIC algorithm (SNR = 10 dB).

Δ_θ	Input (degree)		Output (degree)		RMSE (degree)
2°	30	32	27.83	31.84	1.54
4°	30	34	27.83	33.84	1.54
6°	30	36	28.33	35.35	1.27
8°	30	38	28.33	37.85	1.19
10°	30	40	28.83	39.86	0.83

Table 6: Result of DNN algorithm (SNR = 10 dB).

Δ_θ	Input (degree)		Output (degree)		RMSE (degree)
2°	30	32	29.76	32.43	0.348
4°	30	34	30.23	33.75	0.24
6°	30	36	29.95	35.77	0.166
8°	30	38	30.24	37.75	0.245
10°	30	40	29.98	39.94	0.045

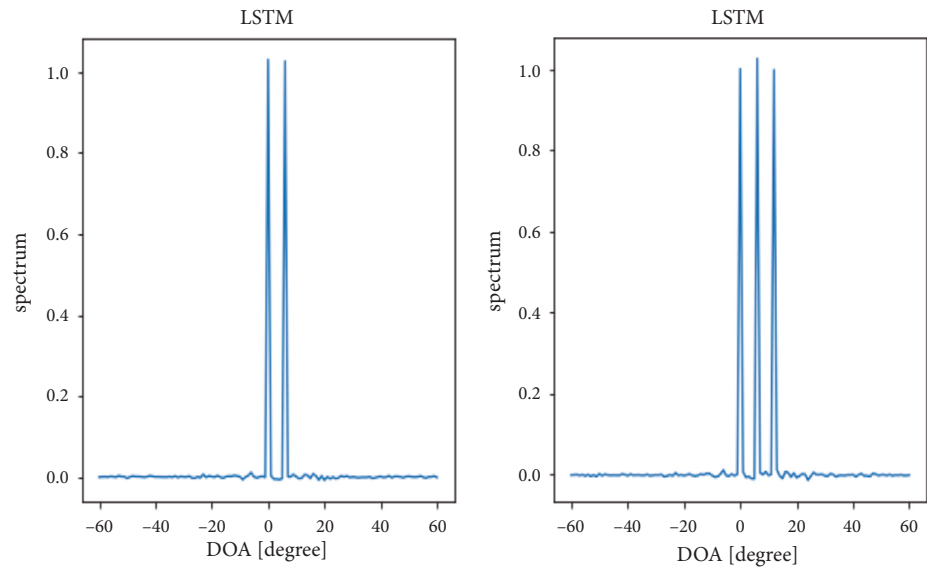

Figure 12: The signal spectrum of the correlated incoming signal based on the LSTM method: (a) 2 signals and (b) 3 signals.

range of [−5 dB ÷5 dB] in the case that the first and second signals are correlated, but they are uncorrelated with the third signal. The received results plotted in this figure shows that the proposed method works better than the other methods. From the above comparison cases, it is easy to see that the LSTM model works effectively and gives good results in most cases, especially in the case of many correlated incoming signals.

Figures 18 and 19 plot the results of the LSTM model in two cases: all three incoming signals are correlated and the case of 2 correlated signals with one uncorrelated signal at SNR = 0 dB and SNR = 5 dB with 31 samples and $\Delta_1 = \Delta_2 = 10^\circ$. It can be easily seen that, in the case of multiple incoming signals, the LSTM model still works well, giving almost accurate results at different SNR values. The comparison results with the MUSIC IMPROVE algorithm in

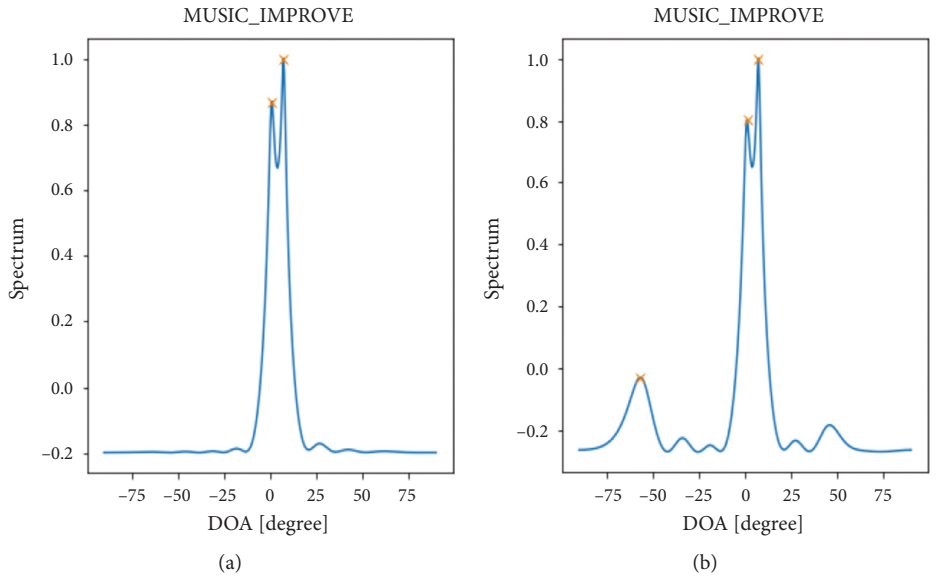

Figure 13: The signal spectrum of the correlated incoming signal based on the MUSIC IMPROVE method: (a) 2 signals and (b) 3 signals.

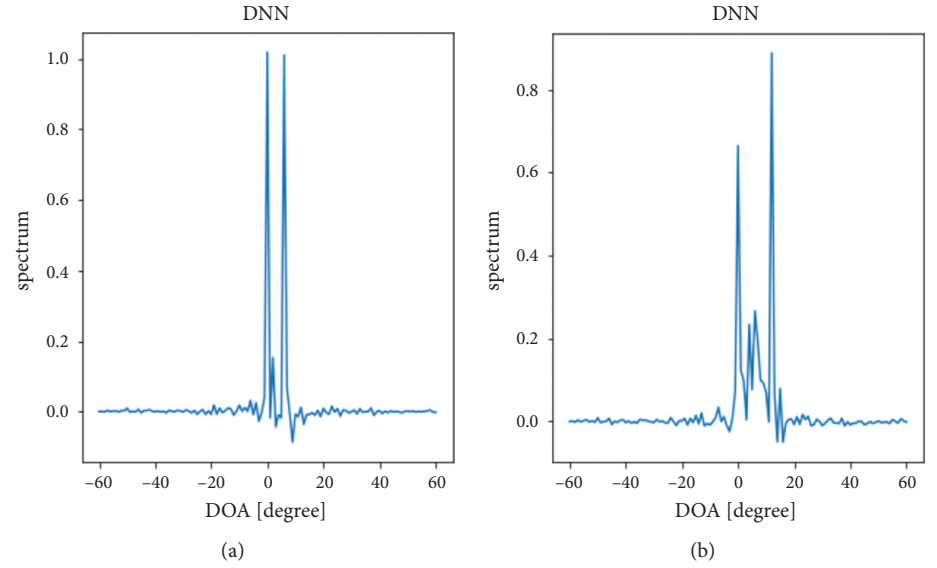

Figure 14: The signal spectrum of the correlated incoming signal based on the DNN method: (a) 2 signals and (b) 3 signals.

Table 7: Results of the LSTM algorithm (SNR = 10 dB).

Δ_θ	Input (degree)			Output (degree)			Result
4	20	24	28	20.58	23.95	27.37	True
6	20	26	32	20.01	26	32.05	True
8	20	28	36	20	28	35.96	True
10	20	30	40	19.99	30	40	True

Table 8: Results of the MUSIC_IMPROVE algorithm (SNR = 10 dB).

Δ_θ	Input (degree)			Output (degree)			Result
4	20	24	28	−30.33	19.08	27.33	False
6	20	26	32	−27.82	21.31	28.83	False
8	20	28	36	−56.46	−4.76	26.32	False
10	20	30	40	−51.40	17.29	26.32	False

Table 9: Results of the DNN algorithm (SNR = 10 dB).

Δ_θ	Input (degree)			Output (degree)			Result
4	20	24	28	20.78	26.34	X	False
6	20	26	32	20	32	X	False
8	20	28	36	19.9	27.65	35.99	True
10	20	30	40	19.83	29.2	39.73	True

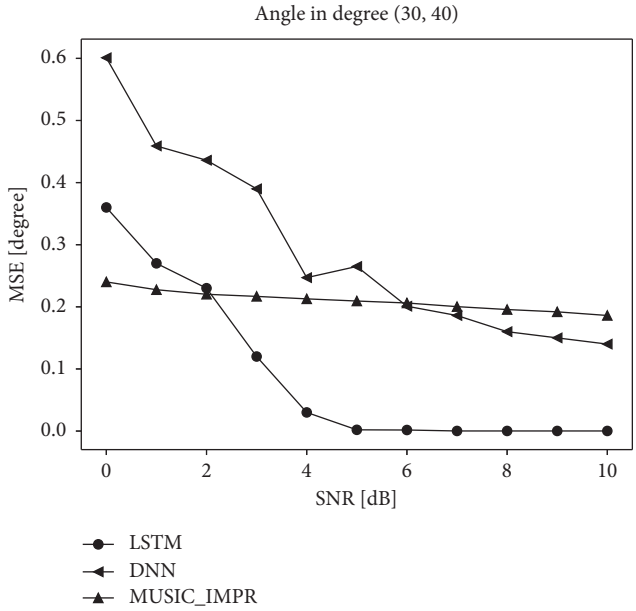

Figure 15: The RMSE (degrees) of the proposed LSTM-based DOA estimation algorithm, the MUSIC-IMPROVE algorithm, and the DNN method with different SNR values.

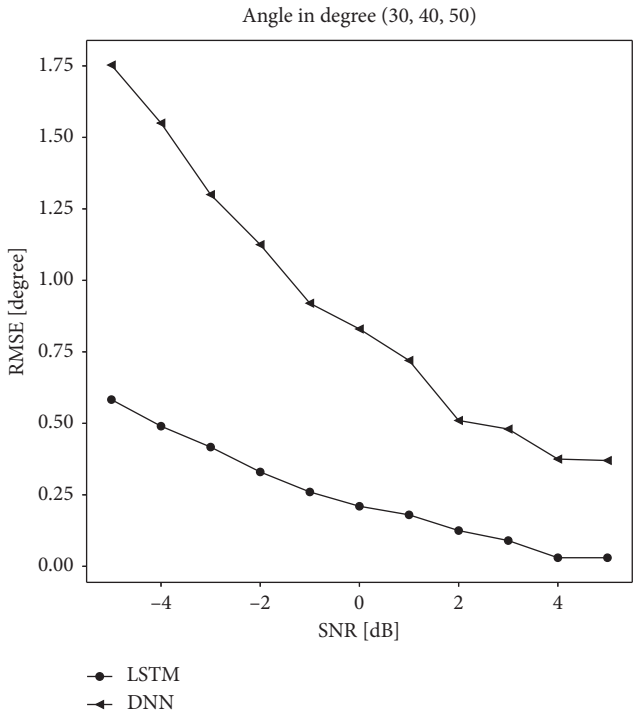

Figure 16: The RMSE (degrees) of the proposed LSTM-based DOA estimation algorithm and the DNN method with different SNR values.

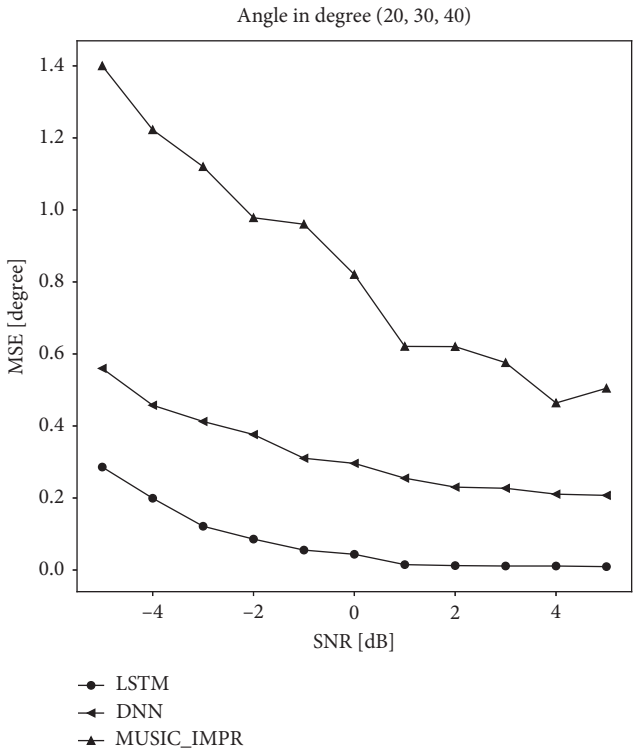

Figure 17: The RMSE (degrees) of the proposed LSTM-based DOA estimation algorithm, the MUSIC-IMPROVE algorithm, and the DNN method with different SNR values.

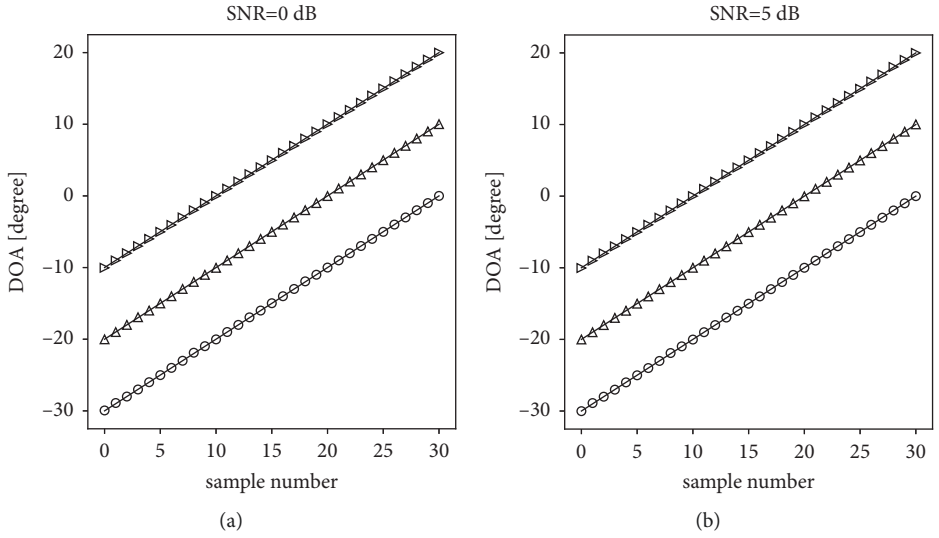

Figure 18: The estimated result of the LSTM method in the case of three correlated incoming signals with $\Delta_1 = \Delta_2 = 10^{\circ}$.

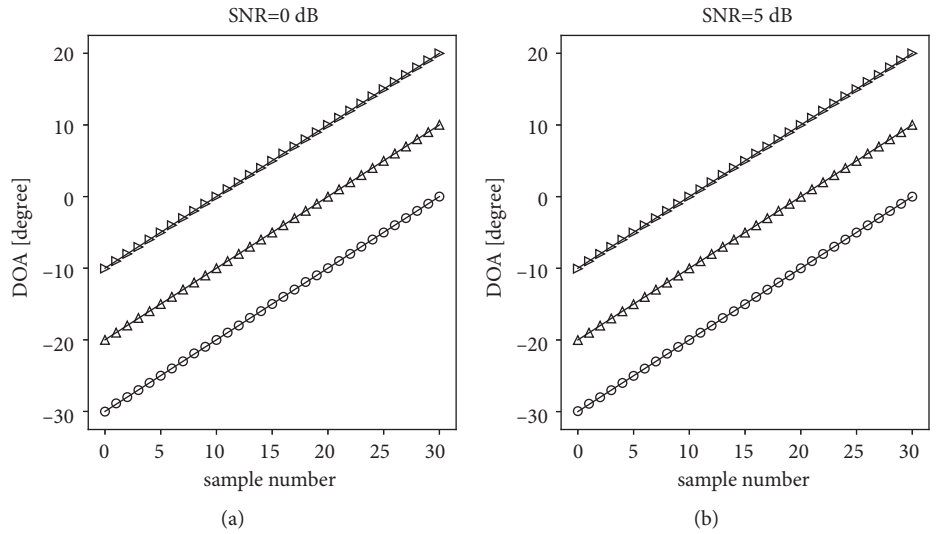

Figure 19: The estimated results of the LSTM method in the case of 2 correlated signals with one uncorrelated signal at $\Delta_1 = \Delta_2 = 10^{\circ}$.

Table 10: Comparison of MUSIC-IMPROVE algorithm and LSTM model.

Simulation cases	LSTM	MUSIC IMPROVE
Signal 1 and signal 2 are uncorrelated	Yes	Yes
Signal 1 is correlated with signal 2	Yes	Yes
Signal 1 and signal 2 are correlated but they are uncorrelated with signal 3	Yes	Yes
All three signals are correlated	Yes	No

the case of correlated signals are also summarized in Table 10.

5. Conclusion

This study proposed the modified LSTM network to estimate the DOA of coherent incoming signals with the ULA antenna system. Two keys contributions of this work are

(i) Create a simulation database of the signal received at the ULA antenna array in the case of multiple incoming sources, which are narrowband signals, in the two cases, where the incoming signals are correlated and uncorrelated

(ii) Propose to apply the modified LSTM algorithm with an architecture that combines network nodes with fully connected layers using Adam's optimization function in the DOA estimation problem in both

cases of uncorrelated and correlated incoming signals

The obtained simulation results show that the model works more accurately than typical algorithms such as MUSIC and DNN algorithms in cases of low SNR, multiple incoming signals, and uncorrelated and correlated incoming signals, as well as when the radiation source is quite close. However, the LSTM algorithm is still limited, where the deviation between the angles is not in the training set and the error is still quite high. In the future, it can be developed to work with other antenna systems, such as UCA, or increase accuracy.

Data Availability

The data used to support the findings of this study are available from the corresponding author upon request.

Ethical Approval

This study was approved by Hanoi University of Science and Technology and Vietnam Maritime University (Vietnam).

Conflicts of Interest

The authors declare no conflicts of interest.

Acknowledgments

The authors appreciate the support from the two universities, Ha Noi University of Science and Technology and Vietnam Maritime University.

References

[1] D. E. Dudgeon and D. H. Johnson, *Array Signal Processing: Concepts and Techniques*, Englewood Cliffs, Bergen County, New Jersey, USA, 1993.

[2] L. Vu Van Yem, *Application of The Music Algorithms to Localisation of Small and Medium-Sized Fishing Boats in Vietnam Sea*, 2007.

[3] B. Ai, C. B. Rodriguez, X. Cheng et al., "Challenges toward wireless communications for high-speed railway," *IEEE Transactions on Intelligent Transportation Systems*, vol. 15, no. 5, pp. 2143–2158, 2014.

[4] Y. Gao, W. Chang, Z. Pei, and Z. Wu, "An improved music algorithm for DOA estimation," *Sensors and Transducers*, vol. 175, no. 7, pp. 75–82, 2014.

[5] D.-S. Kim and V.-S. Doan, "DOA estimation of multiple non-coherent and coherent signals using element," *ICT Express*, vol. 6, pp. 68–76, 2020.

[6] L. Huang, H. Chen, Y. Chen, and H. Xin, "Research of DOA estimation based on music algorithm," in *Proceedings of the 6th International Conference on Machinery, Materials, Environment, Biotechnology and Computer*, Tianjin, China, June 2016.

[7] M. Ahmad and X. Zhang, "Performance of music algorithm for DOA estimation," in *Proceedings of the International Conference in Aerospace for Young Scientists*, China, Beijingpp, 2016.

[8] N. Karmous, M. O. E. Hassan, and F. Choubeni, "An improved esprit algorithm for DOA estimation of coherent signals," in *Proceedings of the International Conference on Smart Communications and Networking*, Yasmine Hammamet, Tunisia, 2018.

[9] H. T. Thanh, V. V. Yem, N. D. Minh, and H. D Thang, *Direction of Arrival Estimation using the Total Forward-Backward Matrix Pencil Method*, ICCE, Virar, India, 2014.

[10] H. T. Thanh, N. T. Chuyen, and N. X. Quyen, "DOA estimation method for CHAOS radar system," *Journal of Science and Technology: Issue on Information and Communications Technology*, vol. 17, 2019.

[11] M. Wajid, A. Kumar, and R. Bahl, "Direction estimation and tracking of coherent sources using a single acoustic vector sensor," *Archives of Acoustics*, vol. 45, no. 2, pp. 209–219, 2020.

[12] M. Chen, Y. Gong, and X. Mao, "Deep neural network for estimation of direction of arrival with antenna array," *IEEE Access*, vol. 8, 2020.

[13] W. Zhu and M. Zhang, "A deep learning architecture for broadband DOA estimation," in *Proceedings of the 19th IEEE International Conference on Communication Technology*, Xi'an, China, 2019.

[14] M. Wajid, F. Alam, S. Yadav, M. A. Khan, and M. Usman, "Support vector regression based direction of arrival estimation of an acoustic source," in *Proceedings of the International Conference on Innovation and Intelligence for Informatics*, Sakheer, Bahrain, 2020.

[15] A. Randazzo, M. A. Abou-Khousa, M. Pastorino, and R. Zoughi, "Direction of arrival estimation based on support vector regression: experimental validation and comparison with music," *IEEE Antennas And Wireless Propagation Letters*, vol. 6, pp. 379–382, 2007.

[16] M. Pastorino and A. Randazzo, "Real-time SVM-based approach for localization of sources," in *Proceedings of the IEEE International Workshop Imaging Systems and Technology (IST)*, Stresa, Italy, 2004.

[17] M. Wajid, F. Alam, S. Yadav, M. A. Khan, and M. Usman, "Support vector machine-based direction of arrival estimation with uniform linear array," *Advances in Computational Intelligence Techniques*, pp. 253–264, 2020.

[18] Z.-M. Liu, C. Zhang, and P. S. Yu, "Direction-of-arrival estimation based on deep neural networks with robustness to array imperfections," *IEEE Transactions on Antennas and Propagation*, vol. 66, no. 12, pp. 7315–7327, 2018.

[19] H. Chung, H. Seo, J. Joo, D. Lee, and S. Kim, "Off-grid DOA estimation via two-stage cascaded neural network," *Energies*, vol. 14, pp. 6–10, 2021.

[20] B. Hu, M. Liu, F. Yi et al., "DOA robust estimation of echo signals based on deep learning networks with multiple type illuminators of opportunity," *IEEE Access*, vol. 8, pp. 14809–14819, 2020.

[21] Y. Yuan, S. Wu, Y. Ma, L. Huang, and N. Yuan, "KR product and sparse prior based CNN estimator for 2-D DOA estimation," *AEU - International Journal of Electronics and Communications*, vol. 137, p. 153780, 2021.

[22] H. Tang, T. Qiu, S. Li, Y. Guo, and W. Zhang, "Robust direction of arrival (DOA) estimation using RBF neural network in impulsive noise environment," *Advances in Neural Networks-ISNN 2005*, vol. 3498, 2005.

[23] R. O. Schmidt, "Multiple emitter location and signal parameter estimation," in *Proceedings of the RADC Spectrum Estimation Workshop*, pp. 243–258, Griffiss AFB, NY, USA, 1979.

[24] G. Bienvenu and L. Kopp, "Principe de la goniometrie passive adaptive," in *Proceedings of the the 7 è me Colloque GRETSI, 106/1-106/10*, Nice, France, 1979.

[25] M. Sugiyama, A. Schwaighofer, N. D. Lawrence, and J. Q. Candela, *Dataset Shift in Machine Learning*, The MIT Press, Cambridge, Massachusetts, USA, 2009.

[26] M. Sugiyama and M. Kawanabe, *Machine Learning in Non-Stationary Environments: Introduction to Covariate Shift Adaptation*, MIT press, Cambridge, Massachusetts, USA, 2012.

[27] L. Wu, Z. M. Liu, and Z. T. Huang, "Deep convolution network for direction of arrival estimation with sparse prior," *IEEE Signal Processing Letters*, vol. 26, no. 11, pp. 1688–1692, 2019.

[28] Y. Kase, T. Nishimura, T. Ohgane, Y. Ogawa, D. Kitayama, and K. Kishiyama, "DOA estimation of two targets with deep learning," in *Proceedings of the 2018 15th Workshop on Positioning, Navigation and Communications*, Bremen, Germany, 2018.

[29] Q. Li, X. Zhang, and H. Li, "Online direction of arrival estimation based on deep learning," in *Proceedings of the IEEE International Conference on Acoustics, Speech and Signal Processing (ICASSP)*, Calgary, AB, Canada, 2018.

[30] M. Wajid, B. Kumar, A. Goel, A. Kumar, and R. Bahl, *Direction of Arrival Estimation with Uniform Linear Array based on Recurrent Neural Network*, in *Proceedings of the 5th IEEE International Conference on Signal Processing, Computing and Control*, Solan, India, 2019.

[31] H. Xiang, B. Chen, M. Yang, S. Xu, and Z. Li, "Improved direction-of-arrival estimation method based on LSTM neural networks with robustness to array imperfections," *Applied Intelligence*, vol. 51, no. 7, 2021.

[32] S. Hochreiter and J. Schmidhuber, "Long short-term memory," *Neural Computation*, vol. 9, pp. 1735–1780, 1997.

[33] M. S. Choi, G. Grosskopf, D. Rohde, B. Kuhlow, G. Przyrembel, and H. Ehlers, "Experiments on DOA-estimation and beamforming for 60 GHz smart antennas," in *Proceedings of the Vehicular Technology Conference Spring*, Jeju, Korea, 2003.

[34] A. H. El Zooghby, G. C. Christos, and M. Georgiopoulos, "A neural network-based smart antenna for multiple source tracking," *IEEE Transactions on Antennas and Propagation*, vol. 48, pp. 1–4, 2000.

[35] D. P. Kingma and B. L. Ba, "Adam: a method for stochastic optimization," 2014, https://arxiv.org/abs/1412.6980.